Article

Ion-Mediated Aggregation of Gold Nanoparticles for Light-Induced Heating

David Alba-Molina, María T. Martín-Romero, Luis Camacho and Juan J. Giner-Casares * iD

Institute of Fine Chemistry and Nanochemistry, Department of Physical Chemistry and Applied Thermodynamics, University of Córdoba, Campus Universitario de Rabanales, Edificio Marie Curie, E-14014 Córdoba, Spain; q32almod@uco.es (D.A.-M.); qf1marot@uco.es (M.T.M.-R.); qf1cadel@uco.es (L.C.)

* Correspondence: jjginer@uco.es; Tel.: +34-957-212423

Featured Application: Photothermal therapy is a highly promising strategy for killing cancer cells and tissues that can be applied in vivo.

Abstract: Photothermal therapy is proposed as a straightforward manner of killing cancer cells, which a plasmon field of gold nanoparticles is activated by incoming light resonance leading to a local increase of temperature. This photothermal effect is strongly dependent on the plasmonic features of the nanoparticles. Herein, we study the effect of the ion-mediated aggregation of citrate-capped small spherical gold nanoparticles on the plasmonic band and the photothermal performance. An intermediate value of ionic strength has been found to be optimum with respect to the photothermal capabilities of the gold nanoparticles.

1. Introduction

Inorganic nanoparticles have opened new avenues of research in biomedicine, where a novel paradigm in therapy and diagnostics in the clinical practice is arising [1]. Plasmonic nanoparticles typically composed of gold or silver appear as a highly promising building blocks due to their photothermal features, among other functionalities. Despite the fact that gold and silver are the most popular metals for fabricating the core of the plasmonic nanoparticles, efficient alternatives can be found using other metals [2]. Photothermal therapy consists of the remote activation of the plasmon field of nanoparticles by irradiation with a resonant light wavelength, leading to a local increase in temperature [3]. This localized heating can kill cancer cells and tissue in an effective manner, with no drugs or biochemical treatment required [4–9].

However, one of the most relevant barriers to be overcome by plasmonic nanoparticles that are to be used in actual clinical treatments is the complex biological media in which the nanoparticles must be dispersed [10]. The ions and biological molecules present in biological media influence the aggregation state of the nanoparticles in most cases, leading to a significant modification of the plasmonic properties of the nanoparticles, which is highly sensitive to interparticle distance [11].

Herein, we aim to determine a fundamental description of the effect of aggregation of gold nanoparticles induced by inorganic ions on the photothermal performance of such nanoparticles. A simplified scenario has been used: small spherical gold nanoparticles coated by citrate ions and sodium chloride as the aggregating-ion. Despite the simplicity of the model, we expect to obtain significant insights that might be used as the first step towards more sophisticated models of nanoparticles and biological media, possibly comprising anisotropic gold nanoparticles capped with different ligands and both inorganic ions and biological macromolecules in the media.

2. Materials and Methods

Materials. Milli-Q water (resistivity 18.2 MΩ·cm) produced by a Millipore Milli-Q unit, pretreated by a Millipore reverse osmosis system, was used in all experiments. Hydrogen tetrachloroaurate trihydrate (HAuCl4·3H$_2$O, ≥99.9%), sodium citrate tribasic dihydrate (≥98%), sodium chloride (≥99.5%), and nitric acid (70%) were purchased from Sigma-Aldrich and used as received. Hydrochloric acid solution (37%) was purchased from Panreac and used as received. All glassware was washed with aqua regia, rinsed three times with Milli-Q water, and dried under a gentle stream of N$_2$ before use.

Synthesis of Nanoparticles. Gold nanoparticle solution comprised an aqueous colloid (average diameter 9 ± 2 nm) that was prepared by adding 5 mL of 1 wt % sodium citrate solution to 95 mL of boiling 0.5 mM HAuCl$_4$ under vigorous stirring. After 15 min of boiling, the solution was cooled down to room temperature and then stored at 4 °C for long-term storage.

Characterization. TEM images were collected with a JEOL JEM-1400PLUS transmission electron microscope operating at 120 kV, using carbon-coated 400 square mesh copper grids. UV–visible spectra of the gold nanoparticles as-synthesized and under different values of ionic strength were recorded in a 1 cm path length disposable cuvette using a Cary 100 Bio UV–visible spectrophotometer.

Photothermal heating experiments. The samples were irradiated using a Xe900 Xenon Arc Lamp (450 W ozone-free xenon arc lamp) from Edinburgh Photonics. The spot of the incoming beam was 1.1 cm, with a circular shape. The irradiation was performed using a constant power density of 1.64 mW/cm^2. The temperature of the bulk solution were monitored along the heating process using an electronic thermometer. The probe of the thermometer was immersed in the bulk dispersion of the nanoparticles. The increase of temperature was found to be very reproducible. The standard deviation between measurements was in all cases equal to or lower than 5%.

3. Results and Discussion

### 3.1. Gold Nanoparticles Capped with Citrate Ions

Gold nanoparticles were synthesized by a modified protocol based on the Turkevich method [12]. A dispersion of citrate-capped spherical gold nanoparticles with a distibution of values of a diameter of 9 ± 2 nm and a polydispersity index (PDI) of 1.51 was obtained, see Figure 1. The polydispersity of the obtained gold nanoparticles was slightly higher than expected from a typical synthesis based on the Turkevich method. We ascribe the higher polydispersity to the presence of impurities in the reaction mixture during the synthesis of the gold nanoparticles. Compared to physical deposition methods, this value of polydispersity is still good. On the other hand, physical deposition methods usually do not suffer from such sensitivity to impurities [13,14]. Note that our study focuses on the plasmonic features of the gold nanoparticle and its activation through incoming resonant light. According to the UV-vis spectra, the plasmon band of the gold nanoparticles is well defined, see Figure 2. Therefore, we assume that the polydispersity of the gold nanoparticle does not play a role in the obtained results of photothermal heating.

During the synthesis of the nanoparticles, the citrate ions act both as reducing and capping agents. Therefore, the surface of the Au nanoparticles is coated by citrate ions attached by electrostatic and non-specific interactions. The gold nanoparticles display a net negative surface charge at the value of pH of the solution used herein. The gold nanoparticles are thus stabilized by charge repulsion [15]. The UV-vis spectrum shows the characteristic peak of small spherical gold nanoparticles at 524 nm, see Figure 2. However, this wavelength value for the plasmon peak is obtained when the gold nanoparticles are dispersed in ultrapure water, a situation significantly different from biological media, which is typically enriched in ions and biological molecules [10]. Therefore, we herein study the plasmonic photothermal features of the gold nanoparticles under different values of ionic strength by adding sodium chloride to the dispersion of gold nanoparticles. We note that the effect of the so-called "protein corona" formation on the gold nanoparticles will not be taken into account [16]. Rather, we

seek a fundamental observation on the effect of aggregation on the photothermal capability of the gold nanoparticles against ionic strength.
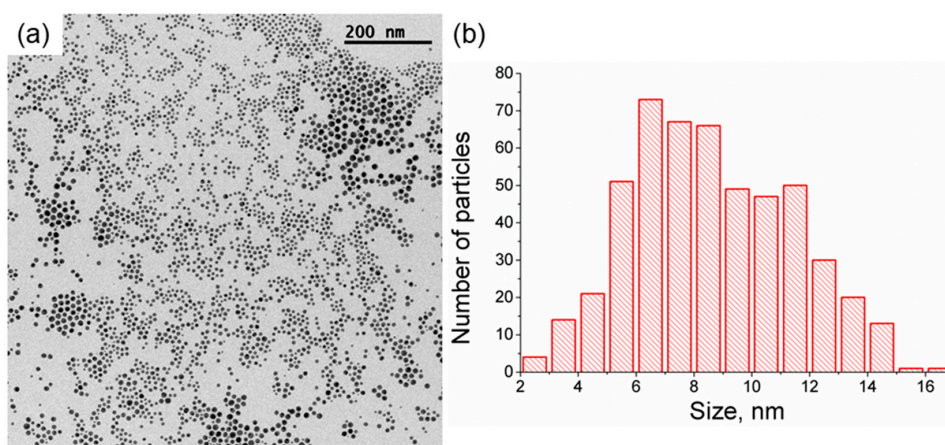
Figure 1. Citrate-capped gold nanoparticles. (**a**) Transmission electron microscopy image of the gold nanoparticles. (**b**) Histogram including the values of size of the gold nanoparticles.
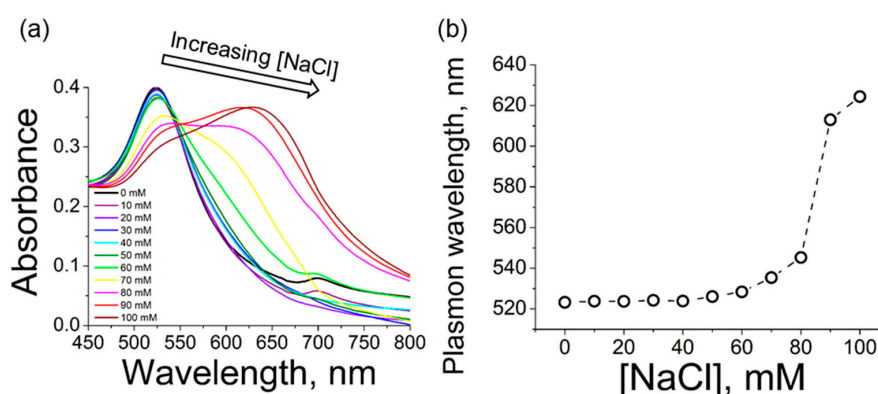
Figure 2. Effect of ionic strength on the plasmon characteristics of the gold nanoparticles. (**a**) UV-vis spectra of the dispersion of gold nanoparticles at different concentrations of sodium chloride from 0 mM (black line) to 100 mM (brown line). (**b**) Values of wavelength corresponding to the plasmon peaks of the gold nanoparticles against ionic strength. The line is included as a guide for the eye.

3.2. Effect of Ionic Strength on the Plasmon Field of the Gold Nanoparticles

With an increase of the ionic strength induced by including sodium chloride and increasing its concentration, the interparticle distance between the gold nanoparticles was effectively reduced [17]. Figure 2 shows the UV-vis spectra for the different values of concentration of sodium chloride up to 100 mM. For higher values of concentration of sodium chloride, irreversible aggregation and loss of gold nanoparticles was obtained. The concentration of gold nanoparticles was estimated using the absorbance at 400 nm [18]. The concentration of gold nanoparticles was ca. 2.7×10^{18} nanoparticles/L in all cases.

There is almost no modification on the plasmon peak of the gold nanoparticles for a sodium chloride concentration up to 50 mM, with a slight shift to higher values of wavelength at 60 and 70 mM of sodium chloride. The plasmon band at 80 mM of sodium chloride displays a different shape with respect to the others, being the limit value for a a change in the tendency of shift of the plasmon band. This modification of the plasmon band, including a broad shoulder at ca. 640 nm, is ascribed to the appearance of large aggregates of nanoparticles. Such aggregation is mediated by the shielding of the repulsive electrostatic interactions of the citrate ions coating the nanoparticles by the sodium

ions in solution. Yet, the more noticeable shift in the plasmon peak occurs at high values of ionic strength, as expected by the enhanced aggregation of the nanoparticles. In this case, a dispersion of gold nanoparticles in 90 and 100 mM of sodium chloride leads to a plasmon peak at ca. 630 nm, see Table 1. Note that, in addition to the significant shift, the plasmon peaks becomes broader at high values of sodium chloride concentration.

Table 1. Values of maximum wavelength for the plasmon peak of the gold nanoparticles ($\lambda_{max,plasmon}$), wavelength of incoming light during photothermal experiments ($\lambda_{irradiation}$), and final increase of temperature during photothermal experiments (ΔT_{max}, standard deviation equal to or lower than 5%) for the different values of ionic strength.

NaCl/mM	$\lambda_{max,plasmon}$/nm	$\lambda_{irradiation}$/nm	ΔT_{max}/°C
0	523	524	1.6
10	523	524	1.8
20	523	524	1.6
30	524	524	1.7
40	524	524	2.1
50	526	525	2.0
60	528	526	1.9
70	535	534	2.0
80	545	575	1.7
90	613	617	1.7
100	624	627	1.9

3.3. Photothermal Experiments

The dispersion of gold nanoparticles was subjected to photothermal experiments by irradiation with a resonant wavelength of light entering the plasmon field of the nanoparticles. The temperature was monitored along the heating process. We note that the measured value of temperature in the bulk solution includes the systematic error of heat dissipation by the environment, especially by the solvent [19]. Therefore, the increase of temperature is compared within the different values of ionic strength. Additional considerations in further studies comprising plasmonic nanoparticles of different sizes and shapes should be included [20].

The wavelength of incoming light was adjusted to the maximum wavelength of the plasmon peak of the nanoparticles, see Table 1. An increase of the temperature of the dispersion of nanoparticles was observed almost immediately after the irradiation begins, see Figure 3. After an irradiation time of ca. 8 min the temperature was not increased further, instead reaching a constant value.
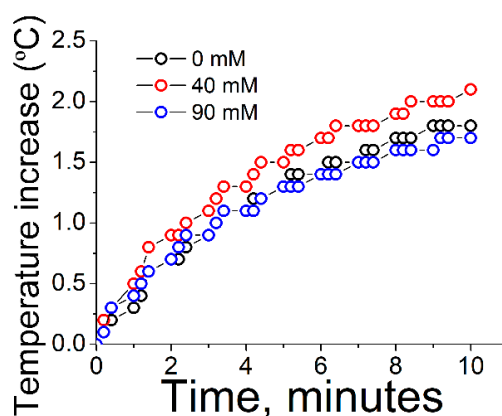
Figure 3. Increase of temperature of the dispersion of nanoparticles against the time of irradiation for different values of sodium chloride concentration: 0 mM (black circles), 40 mM (red circles), and 90 mM (blue circles). The standard deviation between measurements was in all cases equal to or lower than 5%.

The kinetics of photothermal heating was similar in all cases. In a similar study published by Yslas et al., the kinetics of photothermal heating was similar, showing a plateau at ca. 10 min [21]. In that study, the nanoparticles were coated by polyaniline (PANI) polymer. Therefore, we conclude that the kinetics of heating is not determined by the coating of the nanoparticles, but rather by the gold nanoparticles themselves. However, the final value of increase of temperature was slightly but significantly higher for the moderate values of ionic strength, i.e., 40 mM of sodium chloride. This comparatively superior result might be ascribed to a balance between the interplay of two opposite effects. At low values of ionic strength or in the absence of salt, the plasmonic nanoparticles are at a relatively large distance to each other due to the ionic repulsion between the citrate-coated surfaces of the nanoparticles. On the other hand, at high values of ionic strength, the gold nanoparticles are highly aggregated, therefore promoting scattering of the incoming light due to large aggregates, as well as an excessive broadening of the plasmon peak, with both effects contributing to a decrease in the photothermal efficiency.

The intermediate case of ionic strength appears to display a certain aggregation of the plasmonic nanoparticles that promotes the enhancement of the photothermal effect with no excessive aggregation of the nanoparticles. This limited aggregation of the nanoparticles allows for an effective plasmon coupling. Therefore, such an intermediate state of aggregation might be the optimum design when engineering plasmonic nanoparticles for in vivo application of photothermal therapy. The use of highly aggregated nanoparticles with a strongly shifted plasmon field might not yield optimum values in photothermal therapy, despite the interest of higher values of wavelength for biological applications [22].

4. Conclusions

In summary, the photothermal performance of citrate-capped gold nanoparticles at different values of ionic strength has been studied. At low values of ionic strength, the effect of the inorganic ions is not noticeable in the position of the plasmon peak and the photothermal effect. High values of ionic strength lead to strong aggregation of the nanoparticles and large shift in the plasmon position with no net enhancement on the photothermal effect. The optimum scenario for photothermal therapy has been found to be an intermediate value of ionic strength, which allows for a certain aggregation of the plasmonic nanoparticles with no enhanced scattering. The state of aggregation of the plasmonic nanoparticles in the biological media when pursuing applications in photothermal therapy is thus a highly relevant factor in the efficiency of the nanoparticle-based therapy.

Author Contributions: D.A.-M., M.T.M.-R., L.C. and J.J.G.-C. conceived and designed the experiments; D.A.-M.and J.J.G.-C. performed the experiments¸ the paper was written with contributions from all authors.

Conflicts of Interest: The authors declare no conflict of interest.

References

1. Giner-Casares, J.J.; Henriksen-Lacey, M.; Coronado-Puchau, M.; Liz-Marzán, L.M. Inorganic nanoparticles for biomedicine: Where materials scientists meet medical research. *Mater. Today* **2016**, *19*, 19–28. [CrossRef]
2. Lalisse, A.; Tessier, G.; Plain, J.; Baffou, G. Quantifying the Efficiency of Plasmonic Materials for Near-Field Enhancement and Photothermal Conversion. *J. Phys. Chem. C* **2015**, *119*, 25518–25528. [CrossRef]
3. Garcia, M.A. Surface plasmons in metallic nanoparticles: Fundamentals and applications. *J. Phys. D Appl. Phys.* **2011**, *44*, 283001. [CrossRef]
4. Abadeer, N.S.; Murphy, C.J. Recent Progress in Cancer Thermal Therapy Using Gold Nanoparticles. *J. Phys. Chem. C* **2016**, *120*, 4691–4716. [CrossRef]

5. Patino, T.; Mahajan, U.; Palankar, R.; Medvedev, N.; Walowski, J.; Münzenberg, M.; Mayerle, J.; Delcea, M. Multifunctional gold nanorods for selective plasmonic photothermal therapy in pancreatic cancer cells using ultra-short pulse near-infrared laser irradiation. *Nanoscale* **2015**, *7*, 5328–5337. [CrossRef] [PubMed]

6. Khantamat, O.; Li, C.-H.; Yu, F.; Jamison, A.C.; Shih, W.-C.; Cai, C.; Lee, T.R. Gold Nanoshell-Decorated Silicone Surfaces for the Near-Infrared (NIR) Photothermal Destruction of the Pathogenic Bacterium E. faecalis. *ACS Appl. Mater. Interfaces* **2015**, *7*, 3981–3993. [CrossRef] [PubMed]

7. Wang, B.-K.; Yu, X.-F.; Wang, J.-H.; Li, Z.-B.; Li, P.-H.; Wang, H.; Song, L.; Chu, P.K.; Li, C. Gold-nanorods-siRNA nanoplex for improved photothermal therapy by gene silencing. *Biomaterials* **2016**, *78*, 27–39. [CrossRef] [PubMed]

8. Baffou, G.; Quidant, R. Thermo-plasmonics: Using metallic nanostructures as nano-sources of heat. *Laser Photonics Rev.* **2013**, *7*, 171–187. [CrossRef]

9. De Sio, L.; Caracciolo, G.; Annesi, F.; Placido, T.; Pozzi, D.; Comparelli, R.; Pane, A.; Curri, M.; Agostiano, A.; Bartolino, R. Plasmonics Meets Biology through Optics. *Nanomaterials* **2015**, *5*, 1022–1033. [CrossRef] [PubMed]

10. Henriksen-Lacey, M.; Carregal-Romero, S.; Liz-Marzán, L.M. Current Challenges toward In Vitro Cellular Validation of Inorganic Nanoparticles. *Bioconjug. Chem.* **2017**, *28*, 212–221. [CrossRef] [PubMed]

11. Hooshmand, N.; Bordley, J.A.; El-Sayed, M.A. The Sensitivity of the Distance Dependent Plasmonic Coupling between Two Nanocubes to their Orientation: Edge-to-Edge versus Face-to-Face. *J. Phys. Chem. C* **2016**, *120*, 4564–4570. [CrossRef]

12. Enüstün, B.V.; Turkevich, J. Coagulation of Colloidal Gold. *J. Am. Chem. Soc.* **1963**, *85*, 3317–3328. [CrossRef]

13. Ruffino, F.; Crupi, I.; Irrera, A.; Grimaldi, M.G. Pd/Au/SiC Nanostructured Diodes for Nanoelectronics: Room Temperature Electrical Properties. *IEEE Trans. Nanotechnol.* **2010**, *9*, 414–421. [CrossRef]

14. Ruffino, F.; Grimaldi, M.G.; Bongiorno, C.; Giannazzo, F.; Roccaforte, F.; Raineri, V. Microstructure of Au nanoclusters formed in and on SiO$_2$. *Superlattices Microstruct.* **2008**, *44*, 588–598. [CrossRef]

15. Grzelczak, M.; Liz-Marzán, L.M. Colloidal Nanoplasmonics: From Building Blocks to Sensing Devices. *Langmuir* **2013**, *29*, 4652–4663. [CrossRef] [PubMed]

16. Hadjidemetriou, M.; Al-Ahmady, Z.; Kostarelos, K. Time-evolution of in vivo protein corona onto blood-circulating PEGylated liposomal doxorubicin (DOXIL) nanoparticles. *Nanoscale* **2016**, *8*, 6948–6957. [CrossRef] [PubMed]

17. Jain, P.K.; El-Sayed, M.A. Plasmonic coupling in noble metal nanostructures. *Chem. Phys. Lett.* **2010**, *487*, 153–164. [CrossRef]

18. Scarabelli, L.; Grzelczak, M.; Liz-Marzán, L.M. Tuning Gold Nanorod Synthesis through Prereduction with Salicylic Acid. *Chem. Mater.* **2013**, *25*, 4232–4238. [CrossRef]

19. Pallavicini, P.; Basile, S.; Chirico, G.; Dacarro, G.; D'Alfonso, L.; Donà, A.; Patrini, M.; Falqui, A.; Sironi, L.; Taglietti, A. Monolayers of gold nanostars with two near-IR LSPRs capable of additive photothermal response. *Chem. Commun.* **2015**, *51*, 12928–12930. [CrossRef] [PubMed]

20. Maestro, L.M.; Haro-González, P.; Sánchez-Iglesias, A.; Liz-Marzán, L.M.; García Solé, J.; Jaque, D. Quantum Dot Thermometry Evaluation of Geometry Dependent Heating Efficiency in Gold Nanoparticles. *Langmuir* **2014**, *30*, 1650–1658. [CrossRef] [PubMed]

21. Yslas, E.I.; Ibarra, L.E.; Molina, M.A.; Rivarola, C.; Barbero, C.A.; Bertuzzi, M.L.; Rivarola, V.A. Polyaniline nanoparticles for near-infrared photothermal destruction of cancer cells. *J. Nanopart. Res.* **2015**, *17*, 389. [CrossRef]

22. Giner-Casares, J.J.; Henriksen-Lacey, M.; García, I.; Liz-Marzán, L.M. Plasmonic Surfaces for Cell Growth and Retrieval Triggered by Near-Infrared Light. *Angew. Chem. Int. Ed.* **2016**, *55*, 974–978. [CrossRef] [PubMed]